Award Accounts

The Chemical Society of Japan Award for Young Chemists for 2004

Synthesis of Highly Functional Nucleic Acids and Their Application to DNA Technology

Akimitsu Okamoto

Department of Synthetic Chemistry and Biological Chemistry, Faculty of Engineering, Kyoto University, Kyoto 615-8510

Received July 4, 2005; E-mail: okamoto@sbchem.kyoto-u.ac.jp

We have synthesized a number of highly functional nucleic acids and have applied them to DNA technology. Unique characteristics possessed inherently by DNA have been applied to the design of highly functional nucleic acids. We spatially arranged functional bases in the nucleic acid structure, and controlled various functions of the synthetic nucleic acids by changes in sequence, microstructure, and micropolarity. The organic synthesis of such conceptually new functional nucleic acids could open up a new field of genome science and nanobiomaterial science. In this review, we describe the following: (i) rational design of highly functional DNA nanowires, (ii) the development of base-discriminating fluorescent nucleobases and their application to gene polymorphism typing, and (iii) reporter nucleobases for monitoring the change in the microenvironment around DNA and its surroundings.

DNA is an organic biopolymer with a double helix in which bases are arranged in an orderly sequence along sugar–phosphate backbones. It has unique structural characteristics, such as structural transition by external stimulation, base pair formation, and π-stacking of bases. Several applications of DNA to functional materials have recently been developed making good use of these characteristics.[1–3] However, DNA inherently works to transfer genetic information to the next generation and uses only four nucleobases for this purpose. Thus, the possibility of natural DNA to be a functional biomaterial is greatly limited by its small range of functions. Various artificial functional bases should be designed for the development of DNA biomaterials possessing more complicated and controllable functions.

We have created a large number of highly functional DNAs through molecular design and organic synthesis. Various functional bases have been developed and spatially organized in the nucleic acid structure (Fig. 1). Additionally, we were able to activate and suppress various functions depending on sequences, change of microstructure and micropolarity, and modulation of interfunctional interaction. By the appropriate combination of their function control, unique and intelligent functional DNAs have been generated.

Based on this concept, we have studied (i) the rational design and control of DNA wire, (ii) base-discriminating fluorescent nucleobases and their application to a genotyping system, and (iii) the design of functional nucleic acids that sense microenvironmental changes. In this review, we will provide an overview of our recent efforts in the development of highly functional nucleic acids and their application to DNA technology.

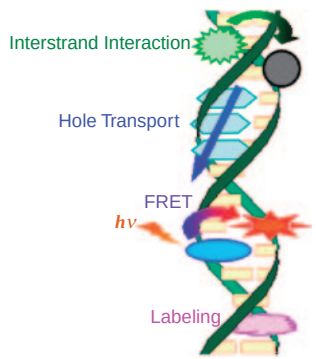

Fig. 1. Schematic illustration of highly functional DNAs prepared through molecular design and organic synthesis. Various functions incorporated into DNA are activated and suppressed depending on sequences and/or changes in microenvironments such as microstructure and micropolarity.

Chemical Approach to Modulating a Long-Range Hole Transport through DNA

In recent years, DNA has attracted a lot of attention as a conductive biopolymer.[4–6] Once a charge is injected into a DNA π-stack, it is able to migrate through the stacked base pair array. Recent efforts to elucidate the mechanism of long-range hole transport in DNA has encouraged us in the respect that DNA can be a good mediator for hole transport by the selection of an appropriate sequence.[7–10] However, when natural DNA is used as a molecular wire, serious unavoidable oxida-

Published on the web December 9, 2005; DOI 10.1246/bcsj.78.2083

tive degradation of G bases occurs. In addition, hole transport in natural DNA is strongly influenced by the sequence and transport distance. Of great importance in the realization of a DNA wire is the molecular design of an artificial nucleobase that can effectively mediate hole transport, while at the same time not be oxidatively decomposed. We herein report on a protocol for designing an artificial nucleobase that can act as an effective mediator for long-range hole transport without subsequent decomposition, and also introduce several applications using the ability to control the hole-transporting efficiency of DNA wires.

G Runs: The HOMO of DNA. G runs in DNA, such as the GG doublet and GGG triplet, are hot spots for oxidative damage caused by hole transport. G runs are also known to be highly susceptible to electrophilic attack by antitumor drugs and mutagens.[11,12] The high reactivity of G runs stems from the stacking of electron-rich G bases, which is reflected in their low ionization potentials. We examined the interaction of G runs with a paramagnetic metal ion by means of ^{15}N NMR using oligodeoxynucleotides (ODNs) containing ^{15}N-enriched G (>98% ^{15}N) at N7.[13] We monitored the change of the ^{15}N NMR spectra by adding $MnCl_2$ to a buffer solution of ODNs containing ^{15}N-labeled GG doublets. Upon increasing the concentration of Mn(II), the broadening of the ^{15}N signals of the 5′G of GG occurred selectively. This binding selectivity was in good agreement with the HOMO distributions in G runs obtained by recent high level MO calculations.[14] Additionally, the line-broadening observed for GGG was larger than that for GG. This is explained in terms of the higher HOMO energy level (i.e., lower ionization potential) of GGG than of GG. The selectivity of G–metal ion interaction (5′-GG $\geq$ GA > GT $\gg$ GC) was also consistent with the order of the HOMO energies of the G sequences (5′-GGG > GG > GA $\gg$ GT, GC).

Rational Design of Highly Functional DNA Nanowires Using ^{BD}A and ^{MD}A. We have designed an artificial nucleobase, benzodeazaadenine (^{BD}A), as a novel efficient hole-transporting nucleobase (Fig. 2).[15] This nucleobase suppressed the oxidative damage caused by the addition of water and/or oxygen to the resulting hole measured as damage in G runs, and increased the hole transport efficiency owing to the enhanced π-stacking arising from the expanded aromatic system.

Long-range hole transport through ^{BD}A-containing DNA was prepared and examined to evaluate the hole transport efficiency and the degree of oxidative degradation of ^{BD}A. The hole transport efficiency was defined by the ratio of oxidative damage at the proximal and distal GGG, as quantified by PAGE. In the reaction of $^{BD}A_5$, a reasonable hole transport value was observed, with no oxidative cleavage of $^{BD}A_5$. In the G runs (i.e., G_5), the hole transport efficiency was relatively low and the DNA was severely damaged at the G_5 site. In addition, the hole transport efficiency decreased by breaking the stacking between the ^{BD}A units.

Based on this result, a ^{BD}A derivative, methoxy-substituted ^{MD}A, was also designed to elucidate the influence of the oxidation potential and the stacking surface area on the hole transport efficiency. Both the ionization potential[12,16] and the base stacking[17] of the bridge sequence have been discussed as important factors for hole transport efficiency through DNA. ^{MD}A has a lower oxidation potential than ^{BD}A, and the stacking surface areas of ^{MD}A, which was obtained from a calculation of the water-accessible surface, is 18% larger than that calculated for ^{BD}A. A hole transport through $^{MD}A_{20}$ (a distance of ca. 7.6 nm) was effectively free to migrate between two GGG sites (Fig. 3). No damage to the $^{MD}A_{20}$ was observed from either PAGE analysis or HPLC analysis after enzyme digestion of photoirradiated DNA. This is quite different from the behavior seen in the G runs. As is needed for a molecular wire, the ^{MD}A run behaved as a good mediator for hole transport and was not oxidatively decomposed.

Amplification of DNA Nanowires by Enzymatic Elongation. DNA is easily extended with DNA polymerases, and amplified up to several million times by means of the polymerase chain reaction (PCR). Much effort in enzymatically incorporating artificial nucleotides using DNA polymerases have been reported in the literature.[18,19] If a method for successive incorporation of ^{MD}A into DNA using DNA polymerases were developed, it would be an efficient technique for the preparation and amplification of molecular wires. We synthesized

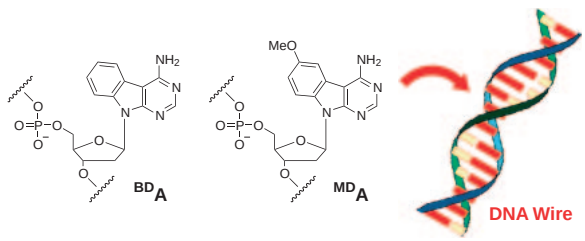

Fig. 2. Hole-transporting nucleotides, ^{BD}A and ^{MD}A. An ^{MD}A run provided an effective DNA wire.

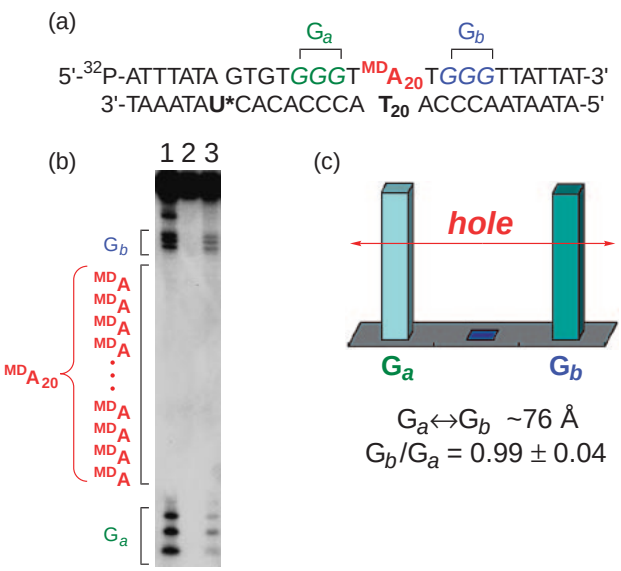

Fig. 3. Effective hole transport through an ^{MD}A run. (a) The sequence of duplex DNA containing $^{MD}A_{20}/T_{20}$. (b) An autoradiogram of a PAGE after photoirradiation of the duplex. Lane 1, Maxam–Gilbert G + A sequencing lane; lane 2, control lane (no photoirradiation); lane 3, photoirradiated duplex DNA. (c) Densitometric analysis of lane 3 of (b). The hole-transporting efficiency obtained from the peak areas of the cleavage bands at both GGG sites was 0.99 ± 0.04.

the 5′-triphosphate salt of ^{MD}A (d^{MD}ATP), and several representative DNA polymerases and reverse transcriptases were examined for d^{MD}ATP incorporation during DNA polymerization.[20] The production of full-length DNA was observed in the polymerization reaction with KOD Dash DNA polymerase. The addition of manganese(II) ions is known to relax the substrate specificity of many DNA polymerases.[21] The synthesis of an ^{MD}A run using a template sequence that included ten successive T nucleotides was accomplished using the polymerization system with KOD Dash polymerase and Mn^{2+}. Because d^{MD}ATP is acceptable to thermophilic DNA polymerase as a substrate under the reaction conditions described above, PCR also acted as a very useful method for the preparation and amplification of ^{MD}A-containing DNA with a high density of hole-transporting units. The PAGE analysis and ESI mass spectrometric analysis of the PCR products supported the production of full-length DNA containing ^{MD}A 10-mer. The extended duplex has a high hole-transporting efficiency, as high as that reported for the ^{MD}A runs above.[15] Thus, the facile synthesis of DNA wires possessing a good hole-transporting ability has been accomplished by the successive incorporation of ^{MD}A using an enzymatic method.

Logic Gates Using DNA Nanowires. A hole-transporting DNA is promising as a new nanoscale electronic device, which is expected to constitute well-regulated bionanomaterials. By combining the hole-transporting ability of the ^{MD}A/T base pair with that of a G/C base pair, the design of molecular logic gates becomes possible. We designed conceptually new molecular logic gates utilizing the hole transport ability of short synthetic DNAs.[22] The key to this system is the orthogonality of the modulation of these hole transport properties by complementary pyrimidine bases. An ^{MD}A/C base pair forms a wobble base pair mediated by a proton or a water molecule, and causes the disruption of π-stacking and the lowering of the HOMO. Therefore, the formation of an ^{MD}A/C base pair was unfavorable for effective hole transport in DNA, and led to the suppression of hole transport. This selectivity is in marked contrast to the selectivity observed for hole transport through G; i.e., a base pair with C is a good hole carrier but a base pair with T strongly suppresses hole transport. If input signals "1" and "0" are applied to T and C, respectively, the hole transport mediated by ^{MD}A will behave like a YES logic and that mediated by G would behave like a NOT logic, which performs inversions. The "logic gate strand," which contained hole-transporting nucleobases (logic bases), such as ^{MD}A and G, was hybridized with the "input strand," which contained pyrimidines that modulate the hole transport efficiency of logic bases (input pyrimidines) (Fig. 4). The hole transport efficiency of the logic gate strand was measured after a phototriggered hole transport reaction. A logic gate strand containing multiple ^{MD}A bases in series provided the basis for a sharp AND logic action. We designed, for example, a logic gate strand containing two ^{MD}A bases in series, which was hybridized with input strands containing different combinations of two input pyrimidines. Hole transport as an output signal was observed when both input pyrimidines for the input strand were T, since hole transport was strongly suppressed when either of the input pyridines was C. For an OR DNA logic gate, we converted the OR equation, "$A + B$," to a standard sum-of-product (SOP) expression, in which all the variables in the domain appeared in each product term.[23] We designed three logic gate strands for OR logic, ^{MD}A–^{MD}A, ^{MD}A–G, and G–^{MD}A, according to each product term in the standard SOP expression for OR logic, and analyzed the hole transport reactions of a mixture of these strands hybridized with an input strand in a single cuvette. In this case, hole transport was not observed only in the case of C–C input. YES, NOT, AND, and OR gates are the basic logic gates from which all logic functions are constructed; therefore, we can easily create complicated logic gates such as NAND, NOR, and XOR in a single cuvette using hole-transporting DNA logic gates. For example, a full adder, which adds three inputs (A, B, and C_{in}) to produce two outputs (Σ and C_{out}) through AND, OR, and XOR operations,[23] was also created according to the protocol. Our DNA logic gate systems, which respond to a given combination of hole transport-controllable base pairs, will open a way for further development encompassing well-regulated molecular electronic devices and biosensors.

Suppression of Hole Transport: ^{AD}A Nucleoside and PNA Strand. The development of an efficient hole-trapping system that can be incorporated into any DNA sequence, regardless of the presence of A/T or G/C base pairs, is very important for the study of long-range hole migration in DNA containing diverse sequences. We developed a highly effective degenerate nucleobase, 2-amino-7-deazaadenine (^{AD}A), which can form stable base pairs with both T and C.[24] ^{AD}A controlled long-range hole migration through an ODN by its unique hole-trapping capacity.[25] The ODNs containing ^{AD}A were cleaved effectively at ^{AD}A regardless of the pyrimidine base with which it was base-paired. The hole-trapping efficiency of ^{AD}A is superior to that of the GGG step and similar to that of 7-deazaguanine (^{Z}G), regardless of the pyrimidine base that base-pairs with ^{AD}A. In addition, a hole can effectively migrate via an ^{AD}A/T base pair, whereas the ^{AD}A/C base pair suppressed hole transport. The reason for the suppression of hole transport by the ^{AD}A/C base pair probably involves the disruption of π-stacking by the formation of a non-Watson–Crick base pair. The hole-trapping efficiency of ^{AD}A varied depending on the base-pairing pyrimidine base.

Peptide nucleic acid (PNA) also acts as an effective inhibitor of hole transport by hybridization to DNA. PNA is a nucleic acid analog possessing a peptide backbone instead of a sugar–phosphate backbone,[26] and is known to tightly bind to complementary DNA and RNA, forming a right-handed duplex.[27] We examined how the efficiency of GG oxidation is altered by hybridization with PNA.[28] In the photooxidation of the DNA/PNA duplex using an oxidant-tethered DNA strand, the efficiency of hole transport in the DNA/PNA duplex was significantly suppressed. The base stacking of the DNA/PNA duplex is significantly different from that in the B-form DNA duplex. In addition, local structural changes also occur not only in the DNA/PNA duplex region, but also at the DNA–PNA junction site as already observed at the DNA–RNA junction.[29] Thus, the change in the electronic overlap of the stacked bases in the DNA/PNA hybrid as a result of structural alterations caused the difference in the hole transport efficiency.

Nucleobase that Releases Reporter Tags upon DNA Oxidation. DNA biosensors offer considerable promise for

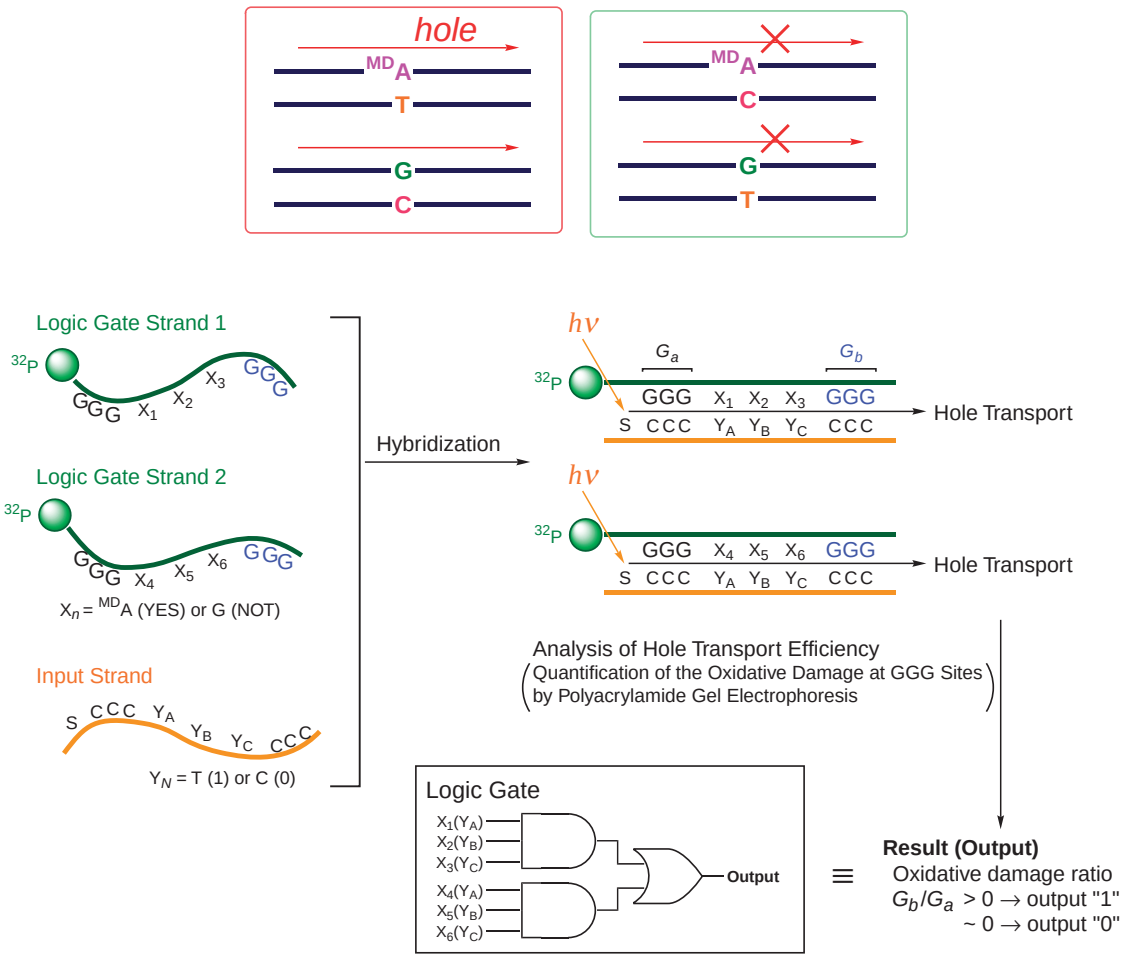

Fig. 4. Modulation of hole transport properties of ^{MD}A and G by complementary pyrimidine bases, and schematic illustration of a DNA logic gate system. The "logic gate strand" (green line), which has "logic bases" (X_n), such as ^{MD}A and G, was hybridized with the "input strand" (orange line), which contains "input pyrimidines" (Y_n) opposite logic bases. The duplex also includes a photosensitizer S for hole injection to DNA and two GGG sites for hole detection. Hole transport is triggered by photoirradiation with a transilluminator (312 nm) at 0 °C. The hole transport efficiency of the logic gate strand as an output is defined by the ratio of oxidative strand cleavage at both GGG sites (G_b/G_a).

extracting information from target genes in a quick and simple manner. A molecular releasing system that is triggered by external stimulation such as oxidation or photoirradiation would be a useful tool for gene analysis. We developed a novel nucleoside, ethylenediamine-modified G (^{eda}G), and a new molecular releasing system controllable by the one-electron oxidation of ODNs (Fig. 5).[30] The method using ^{eda}G constitutes a facile strategy for detecting long-range hole transport through DNA without complicated and unwieldy analysis processes such as quantification of oxidative guanine damage of labeled DNA or the analysis of photodynamics. ^{eda}G was incorporated into ODNs by a conventional method, and the reporter units were incorporated into the amino side chain of ^{eda}G in the ODNs by the post-synthetic modification of ^{eda}G-containing ODNs using the *N*-hydroxysuccinimidyl esters of carboxylic derivatives such as benzoic acid and tetramethylrhodamine (TAMRA).

We examined the detection of TAMRA released from ODNs containing a TAMRA-tethered ^{eda}G via long-range hole transport through DNA. A strong fluorescence at 576 nm was observed from the sample after photoirradiated long-range hole transport. The fluorescence intensity of the sample increased in proportion to the irradiation time. ^{eda}G acts as a very efficient hole trap, and the hole in the duplex is selectively trapped at the ^{eda}G site via a long-range hole transport to result in the release of TAMRA from the duplex. The products after the oxidative degradation, the ODN with an abasic site and the reporter tag possessing a guanidinium group, strongly suggest that the rapid decomposition of ^{eda}G may proceed via the G cation radical decomposition mechanism proposed earlier[31,32] resulting in the release of a reporter tag. Reporter units tethered to ^{eda}G were easily released from ODNs by mild oxidation. In a long-range hole transport experiment, a DNA duplex containing ^{eda}G efficiently and stoichiometrically released a fluorescent tag.

Hole-Transporting DNA Duplex Immobilized on a Gold Electrode. Molecular engineering of artificial self-assemblies with desired functions on a surface has attracted a lot of interest as an advancement of nanotechnology. Self-assembled monolayers are good candidates for a stable and effective pho-

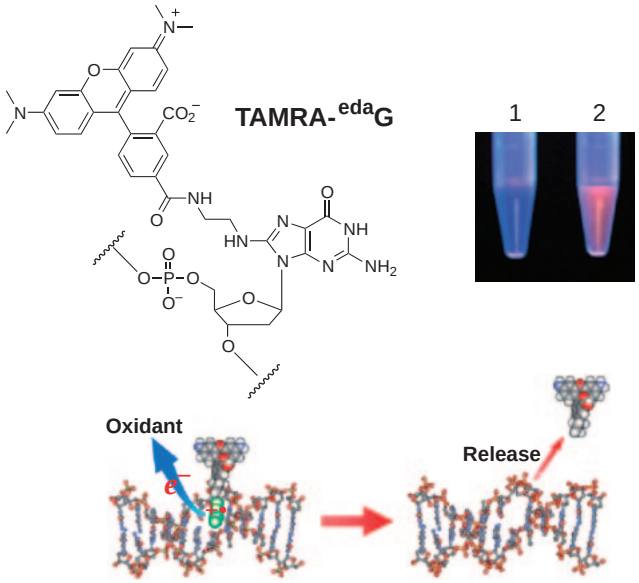

Fig. 5. TAMRA-edaG that efficiently releases TAMRA upon one-electron oxidation. The image is the fluorescence of the samples obtained by filtration after photoirradiation of the control duplex (sample 1) and the duplex containing a photosensitizer (sample 2).

toelectrochemical device for light-initiated electron transfer.[33–35] The construction of well-organized hole-transporting DNA assemblies on a solid surface would produce a photocurrent arising from photostimulated hole transport through DNA. Based on this concept, we prepared a thiolated DNA strand and an anthraquinone-labeled complementary strand (Fig. 6).[36] Subsequently, mixed monolayer surfaces containing a thiolated DNA and 6-mercapto-1-hexanol were prepared by immersing a gold electrode in solutions of thiolated DNA and then 6-mercapto-1-hexanol. By hybridization with the anthraquinone-labeled complementary DNA, the DNA duplex was assembled on the surface of a gold electrode. Photoelectrochemical measurements on the photosensitizer-labeled duplex-modified gold electrode were carried out using 365 nm light at an applied potential of 500 mV versus SCE. A stable cathodic photocurrent appeared immediately upon irradiation of the modified gold electrode. In contrast, the photocurrent dropped instantly when the illumination ceased. The cathodic photocurrent increased sharply with increasing positive bias on the gold electrode. This indicates that the generation of photocurrent was controlled by positive charge transport, i.e., hole transport between the gold electrode and the DNA. The dark current on the gold electrode remained almost constant within the applied potential range. After bubbling argon through the solution, the observed photocurrent decreased. Oxygen acts as an effective electron carrier from the reduced anthraquinone in the present system, and leads to higher current densities. The efficiency of photostimulated hole transport through the DNA duplexes on the gold electrodes was strongly affected by the duplex sequences. The bridged sequence taking part in the G-hopping strongly influenced the photocurrent density, and the decrease in current density shows that a G base is necessary for efficient hole transport on the gold surface. The observed photocurrent was also suppressed of an electrode modified by a duplex containing a G/T mismatched base pair. The disruption of the π-stacking array by the G/T mismatch strongly influenced the photocurrent intensity, i.e., the photocurrent intensity was regulated by the replacement of the complementary strand. By modifying a gold electrode with a DNA duplex containing a photosensitizer, we observed a sequence-dependent cathodic photocurrent. Photoinitiated hole-transporting DNA molecules immobilized on a solid surface will facilitate the development of a variety of nanobiotechnological applications, from biosensors to photosynthetic model systems.

Single Base Discrimination by Fluorescent Deoxynucleosides and Oligodeoxynucleotides

Base-Discriminating Fluorescent Nucleobases. The importance of DNA sequence identification is increasing as our knowledge of the association between genotypes and phenotypes accumulates. Recently, there has been growing interest in single nucleotide polymorphisms (SNPs), which are single base-pair substitutions that occur within and outside genes.[37,38] The typing of SNPs using DNA probes is a rapidly developing area. Most of the presently available methods utilize the difference in hybridization efficiency between the target DNA and the probe ODNs,[39–42] or the difference in enzymatic recognition between full-matched and mismatched duplexes.[43–46] However, there are still problems, such as hybridization errors, the high cost of enzymes, and the time-consuming steps required. The differences in the hybridization efficiencies vary with sequence context, and the efficiency is often too small for the detection of a single base mismatch in long target strands of DNA. Provided that the detection method relies on hybridization events, such DNA probes have inherent limitations in their selectivity. DNA probes labeled by well-designed fluorophores will have the potential to simplify DNA probe assays if the fluorescence label exhibits a drastic change in fluorescence intensity when the labeled probe hybridizes with a target sequence.

At present, many fluorophores, such as fluorescein, Alexa dyes, and cyanine dyes, have been developed, and several analyzers and imagers that have been adjusted to the emission wavelength of these fluorophores are commercially available. However, the fluorescence of these known fluorophores is relatively insensitive to conjugated DNA sequences, with the exception that it is often decreased by a G base located in the neighborhood of an attached fluorophore.[47,48] Such fluorophores are unsuitable for direct detection of a small change in the DNA microenvironment.

We have recently demonstrated a new concept for designing base-discriminating fluorescent (BDF) nucleobases, which can clearly distinguish the type of base opposite the BDF base by a change in fluorescence (Fig. 7). This concept could be very important and useful for devising new SNP typing methods. Due to the fluorescence change of BDF nucleobases, the bases on complementary strands can be fluorometrically read without separation and washing. Therefore, our SNP typing method using BDF probes constitutes a very powerful homogeneous assay that does not require enzymes or time-consuming steps and avoids hybridization errors.

Size-Expanded BDF Nucleosides: We initially devised a new fluorescent nucleoside, benzopyridopyrimidine (BPP),[49]

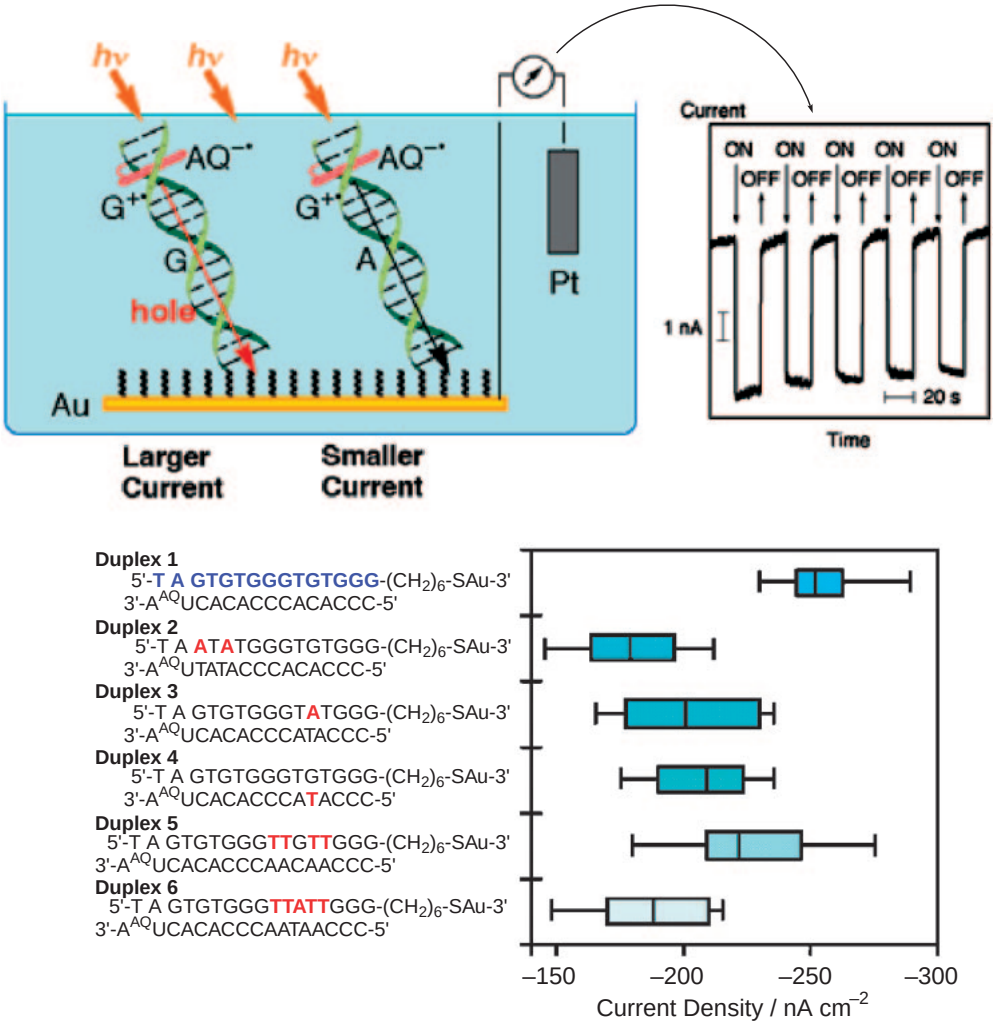

Fig. 6. Measurement of a photocurrent using a gold electrode modified with an anthraquinone-modified DNA duplex. Photoelectrochemical response data of the duplex-modified gold electrode irradiated with 365 nm light at 13.0 mW cm^{-2} with a 500 mV bias versus SCE are shown.

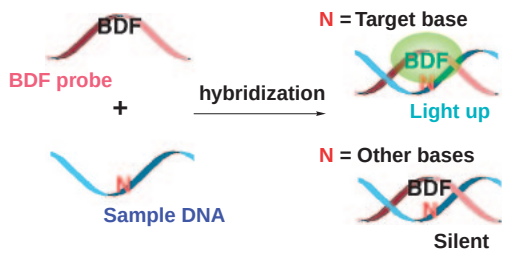

Fig. 7. Schematic illustration of a new homogeneous SNP typing method using a base-discriminating fluorescent (BDF) probe. BDF probes give strong fluorescence only when the base opposite the BDF base is a target base.

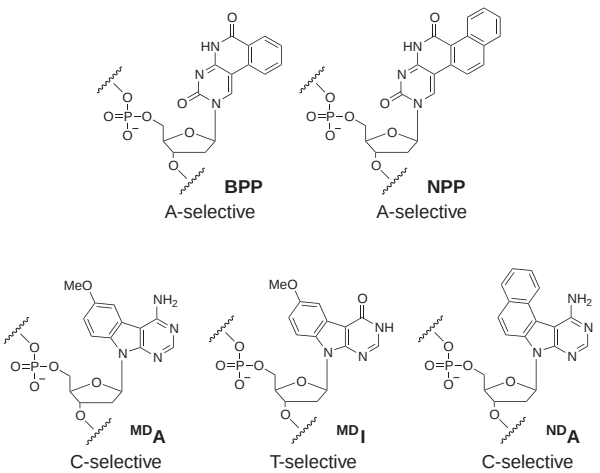

Fig. 8. Structures of size-expanded BDF nucleosides.

that can distinguish purine bases on complementary strands (Fig. 8). The fluorescence behavior of the BPP-containing ODN, 5′-d(CGCAAT[BPP]TAACGC)-3′, was strongly dependent on the purine bases opposite BPP. The fluorescence spectra of the duplex formed by hybridization with 5′-d(GCGTTA**A**ATTGCG)-3′ had a fluorescence peak at 390 nm (Φ_F = 0.035), whereas the fluorescence of the duplex formed by hybridization with 5′-d(GCGTTA**G**ATTGCG)-3′ was almost completely quenched (Φ_F = 0.0018). It was confirmed from melting temperature (T_m) measurements of the duplex and the

^{15}N NMR of ODNs containing [3-^{15}N]- and [4-^{15}N]-enriched BPP that BPP is an effective degenerate base, forming stable base pairs in the Watson–Crick pairing mode for BPP/G and in the wobble mode for BPP/A. The fluorescence decay study strongly suggests that tight hydrogen bonds between BPP as a fluorophore and G as a quencher form a complex that undergoes an extremely rapid quenching, and results in an effective quenching of the BPP fluorescence. The clear change in fluorescence that depends on the type of purine base opposite BPP will be very useful for SNP typing of genes. We tested the ability to distinguish purine bases by BPP hybridization on the A/G SNP sequence of the human interferon-γ gene (IFNG).[50] As a result, a strong visible emission was obtained with the A-allele duplex, 5′-d(CCACAT[BPP]TTATGA)-3′/5′-d(TCATAAA**A**ATGTGG)-3′, whereas the emission from the G-allele duplex, 5′-d(CCACAT[BPP]TTATGA)-3′/5′-d(TCATAA**G**ATGTGG)-3′, was negligible (Fig. 9). The hybridization of BPP-containing ODN with a target DNA facilitates judgment by naked eye recognition of the type of purine located at a specific site on the target DNA. However, the general utility of this method is limited by the flanking base pair of BPP. When the flanking base pair is a G/C base pair, the fluorescence of BPP is significantly suppressed.[51] Although there is such a limitation, A-selective fluorescence emission using BPP is also effective for identifying the type of purine bases located at a specific site on RNA.[52]

Furthermore, we designed a larger size-expanded BDF nucleoside, naphthopyridopyrimidine (NPP).[53] The base selectivity of the fluorescence emission of NPP was very similar to the selectivity observed for BPP, but the quantum yield of NPP hybridized with an adenine base was greatly enhanced ($\Phi_F = 0.096$), as compared with that of BPP hybridized with an adenine base ($\Phi_F = 0.035$).[49] The fluorescence of NPP hybridized with a guanine base is still very weak ($\Phi_F = 0.007$ for NPP and 0.0018 for BPP). The hybridization of an NPP BDF probe with a target DNA facilitates judgment of the type of purine base located at a specific site on the target DNA, and is very effective for A/G SNP typing.

We also devised novel fluorescent size-expanded nucleosides, methoxybenzodeazaadenine (^{MD}A) and methoxybenzodeazainosine (^{MD}I), which emit strong fluorescence only when the base on the target strand is C and T, respectively.[54] The fluorescence intensities of the single-stranded 5′-d(CGCAAT-^{MD}ATAACGC)-3′ ($\Phi_F = 0.005$) and the duplex formed by hybridization with 5′-d(GCGTTA**T**ATTGCG)-3′ ($\Phi_F < 0.0005$) were very weak. However, the fluorescence spectrum of the duplex formed by the hybridization with 5′-d(GCGTTA**C**ATTGCG)-3′ showed a strong fluorescence at 424 nm ($\Phi_F = 0.081$). In contrast, when 5′-d(CGCAAT^{MD}ITAACGC)-3′ was hybridized with 5′-d(GCGTTA**T**ATTGCG)-3′, a relatively strong fluorescence was observed at 424 nm ($\Phi_F = 0.011$) that was 5.5 times stronger than that observed for the duplex formed by hybridization with 5′-d(GCGTTA**C**ATTGCG)-3′ ($\Phi_F = 0.002$). By means of BDF probe hybridization, we tested the SNP detection of the T/C SNP sequence of the human breast cancer 1 gene (BRCA1). BDF probes, 5′-d(GGTACC-A^{MD}ATGAAATA)-3′ and 5′-d(GGTACCA^{MD}ITGAAATA)-3′, were mixed with a sample solution of the target sequences, 5′-d(TATTTCA**T**TGGTACC)-3′, 5′-d(TATTTCA**C**TGGTA-CC)-3′, or a 1:1 mixture of them to mimic the heterozygous state, and the fluorescence of the mixture was immediately read at room temperature with a fluorescence imaging instrument. As a result of the hybridization of the target BRCA1 sequences with the BDF probes, three types of sample were clearly distinguished by the measurement of their fluorescent intensities.

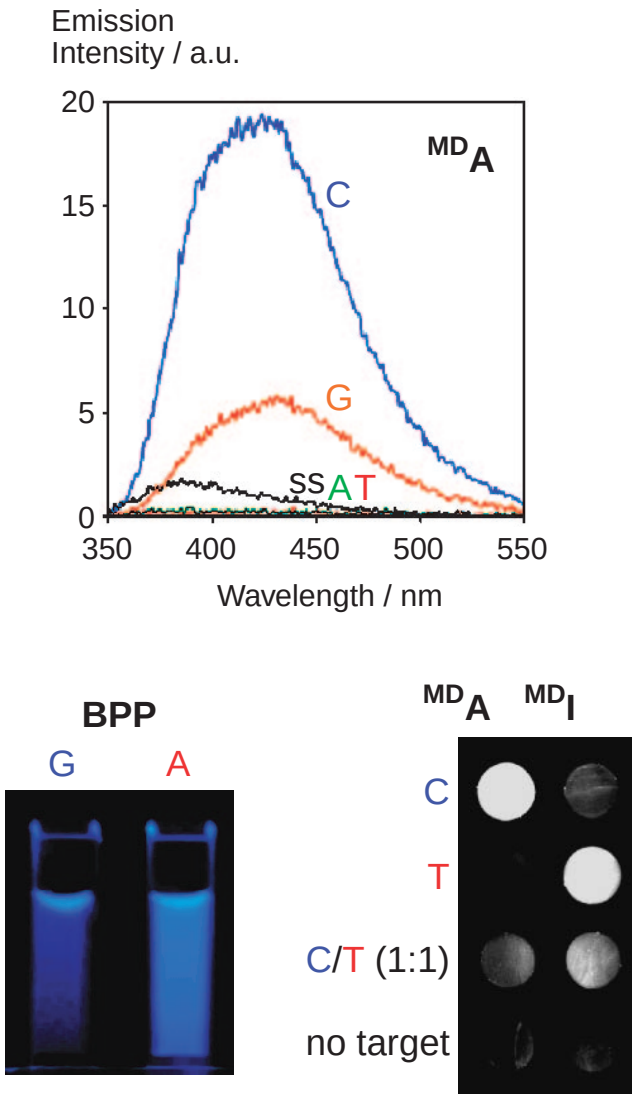

Fig. 9. Change in fluorescence intensities by the base pair formation of BDF bases with different bases. (top) C-selective fluorescence of ^{MD}A in 5′-d(CGCAAT^{MD}ATAA-CGC)-3′/5′-d(GCGTTA**N**ATTGCG)-3′ (N = C, G, T, or A). (bottom, left) Determination of the A/G allele type of the human interferon-γ gene using the change of BPP fluorescence. (bottom, right) Determination of the T/C allele type of BRCA1 using the fluorescence change of ^{MD}A and ^{MD}I BDF probes.

The fluorescence behavior of BDF nucleosides has a remarkable advantage that is not observed for the commonly used fluorophores. However, the fluorescence wavelength of the BDF nucleosides is slightly shorter than that used by commercially available DNA fluorescence analyzers. By using

fluorescence resonance energy transfer (FRET) from naphthodeazaadenine (NDA), which shows a fluorescence emission only when the base opposite NDA is C, to fluorescein, a strong emission from fluorescein was observed only when the base opposite NDA was C.[55] Since the fluorescence emission spectrum of NDA overlapped with the fluorescence excitation spectrum of fluorescein in the wavelength range of 400–500 nm, the interaction of these two fluorophores that are separated by defined base pairs allows an efficient energy transfer to result in a dominant fluorescence emission of fluorescein at 520 nm by excitation at 350 nm. We designed a series of FRET-BDF probes containing NDA as the FRET donor and fluorescein as the acceptor that were separated by three A/T base pairs. The fluorescence emission from the duplex, 5′-d(FAATNDATA-ACGCACACG)-3′/5′-d(CGTGTGCGTTA**C**ATT)-3′ (F = 6-(fluorescein-6-carboxamido)hexanol) was observed selectively, and the quenching efficiency (Q_F) of NDA was 83%. In contrast, hybridization of the FRET-BDF probe with 5′-d(CGT-GTGCGTTA**N**ATT)-3′, where N is T, G, or A, resulted in a weaker emission. By using FRET-BDF probes containing both NDA and fluorescein, the C-selective fluorescence of NDA was transferred to fluorescein. This system facilitates the detection of a single nucleotide alteration in a target sequence at the wavelength of the fluorescein emission.

Pyrene-Labeled BDF Nucleosides: Although the ODNs containing BDF bases are actually used as tools for the detection of single nucleotide alterations, there are still problems to be solved, such as the quenching of the BDF fluorescence by the flanking G/C base pairs. An SNP typing method employing such a BDF base would be inaccurate for a sequence containing a G/C base pair near the SNP site. Thus, a new type of BDF base that is more base-selective and insensitive to flanking base pairs is highly desirable.

We designed pyrene-labeled nucleosides, ^{Py}U, which possess pyrenecarbonyl fluorophores attached to uracil bases at the C-5 position via a rigid propargyl linker (Fig. 10).[56] The fluorescence of pyrene-1-carboxaldehyde is very strong in polar solvents due to the preferred π–π^* transition.[57] By using such fluorescence changes, it becomes feasible to experimentally sense the nucleobases opposite the BDF base in a target strand. ^{Py}U exhibited unique fluorescence properties depending on the nature of the base on the complementary strand. The fluorescence spectrum of the ^{Py}U/A duplex showed a strong fluorescence at 397 nm following 327 nm excitation. In contrast, the fluorescence of the single-stranded state and mismatched duplexes was much weaker. The base-selective fluorescence emission for the ^{Py}U-containing duplex strongly correlates with the polarity sensitivity of the ^{Py}U fluorophore. In the energy-minimized structures for the duplex containing a ^{Py}U/A base pair, the pyrenecarboxamide chromophore of ^{Py}U was extruded to the outside of the duplex and exposed to a highly polar aqueous phase (Fig. 11). On the other hand, the duplex containing a ^{Py}U/G mismatched base pair showed a structure in which the glycosyl bond of uridine was rotated to the *syn* conformation. The propargyl linker of ^{Py}U was stacked into the minor groove and the pyrenecarboxamide unit was bound to the duplex along the minor groove. In this conformation, the pyrenecarboxamide group was located at a hydrophobic site of the duplex. In addition, the advantage of the use of ^{Py}U as a BDF base is that the fluorescence was not quenched by the flanking C/G base pair as observed for 5′-d(CGCAA-C^{Py}UCAACGC)-3′/5′-d(GCGTTG**A**GTTGCG)-3′, probably because the rigid propargyl linker keeps the fluorophore apart from the flanking Gs. These fluorescence properties are quite different from those observed in size-expanded BDF nucleo-

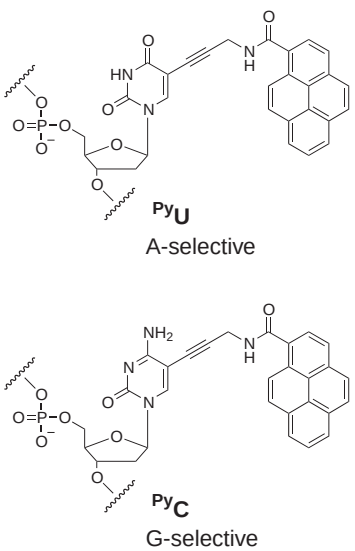

Fig. 10. Structures of pyrene-labeled BDF nucleosides.

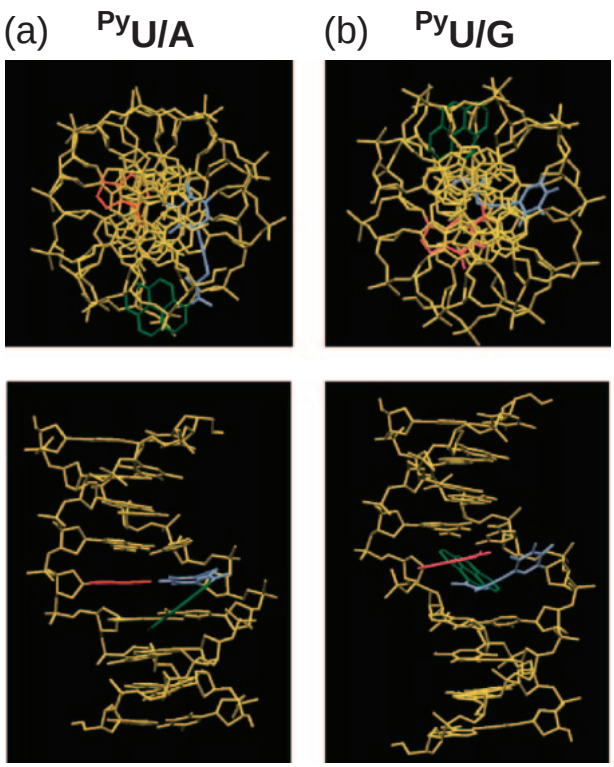

Fig. 11. Simulated conformations of duplexes 5′-d(AAA-C^{Py}**U**CAAA)-3′/5′-d(TTTG**N**GTTT)-3′. (a) **N** = A. (b) **N** = G. Top views (top) and side views from the major groove (bottom) are shown. ^{Py}**U** and the complementary **N** base are represented by blue and red, respectively. The pyrene group of ^{Py}**U** is shown in green.

bases where the fluorescence is efficiently quenched by flanking C/G base pairs. Because ^{Py}U shows a highly A-selective fluorescence emission, we also designed the analogous C derivative (^{Py}C), which exhibits a G-selective fluorescence emission. The fluorescence emission from 5′-d(CGCAAC^{Py}CCAACGC)-3′/5′-d(GCGTTGNGTTGCG)-3′ was highly G-selective. A BDF nucleoside that emits fluorescence selectively for G is unusual, and ^{Py}C is the first BDF nucleoside that can detect a G base on the complementary strand.

A fluorescence change induced by the nature of a complementary base would be very useful for SNP typing. For example, we examined the discrimination of SNPs in the human H_a-*ras* SNP sequence,[58] which possesses a C/A SNP site, using ^{Py}U-containing BDF probes. On hybridization of a ^{Py}U-containing BDF probe, 5′-d(GGCGCCG^{Py}UCGGTGTG)-3′, with the target sequence, the ^{Py}U probe showed an A-allele-specific fluorescence at 398 nm. The fluorescence of a non-hybridized ODN or an ODN probe hybridized with a C-allele sequence was negligible. The homogeneous SNP typing method using pyrene-labeled BDF probes would be a powerful alternative to conventional SNP typing methods.

Pyrene-Labeled Probe for Detecting Insertion Mutations. Insertion/deletion (indel) polymorphisms constitute approximately 10% of all the polymorphisms in the human genome,[38] and lead to serious gene expression errors because they often cause a translational frameshift and create premature proteins. It is very desirable to develop a new ODN probe that can easily determine indel polymorphisms at a specific site on the target DNA. Pyrene-labeled ODN is expected to be a candidate for such an ODN probe for indel polymorphism detection. Excimer formation and the intercalating ability of the pyrene chromophore will facilitate the detection of an extra base in target DNA. Based on this concept, we designed a ^{Py2}Lys backbone-containing ODN, 5′-d(GTGTTAAGCC^{Py2}LysGCCAATATGT)-3′ (Fig. 12).[59] When the ^{Py2}Lys-containing ODN was hybridized with 5′-d(ACATATTGGCGGCTTAACAC)-3′, which does not possess the base opposite ^{Py2}Lys, the fluorescence was weak ($\Phi_F = 0.007$) following excitation at 350 nm. In contrast, the fluorescence spectrum of the duplex with 5′-d(ACATATTGGC**A**GGCTTAACAC)-3′, where A is the base opposite ^{Py2}Lys, had a strong fluorescence peak at 495 nm ($\Phi_F = 0.088$), corresponding to the fluorescence wavelength from a pyrene excimer. The fluorescence from the probe was almost constant regardless of the nature of the base opposite ^{Py2}Lys. On the other hand, the fluorescence behavior of the ^{Py2}Lys-containing ODN was dependent on the number of inserted bases. With an increase in the number of bases opposite ^{Py2}Lys in the duplexes such as 5′-d(ACATATTGGC(**A**)$_n$GGCTTAACAC)-3′ ($n = 1$–3), the fluorescence intensity gradually decreased.

A clear change in fluorescence that depends on the presence/absence of an inserted base opposite ^{Py2}Lys is very useful for the detection of insertion polymorphisms. We tested the detection of an insertion mutation by the hybridization of the ^{Py2}Lys-containing probe using the coding sequence of the epithelial sodium channel β subunit (βENaC) gene associated with Liddle's syndrome, which is an autosomal dominant form of hypertension with variable clinical expression.[60,61] We prepared the ^{Py2}Lys-containing probe, 5′-d(CTCACTGGGGTAG-

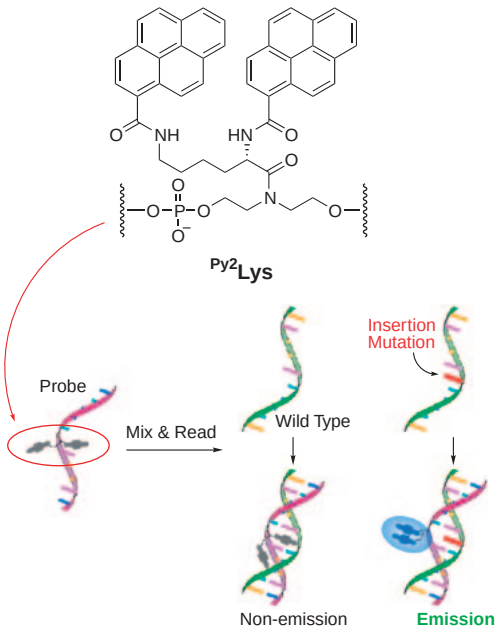

Fig. 12. Schematic illustration of a new method for indel polymorphism detection using ODN probes containing two pyrene chromophores (^{Py2}Lys).

GGCCCAGT^{Py2}**Lys**GTTGGGGCT)-3′, and hybridized with βENaC gene sequences, 5′-d(AGCCCCAAC(**G**)$_n$ACTGGGCCCTACCCCAGTGAG)-3′ (wild type, $n = 0$; G-inserted mutant, $n = 1$). The fluorescence emission from the duplex with a G-inserted strand was very strong and clearly distinguishable from the poor fluorescence of the duplex with a wild-type strand. The hybridization of the ^{Py2}Lys-containing ODN with a target DNA facilitates the determination of the presence/absence of insertion polymorphisms located at a specific site on the target DNA.

Sequence-Selective Discrimination between Cytosine and 5-Methylcytosine. 5-Methylcytosine (^{m}C) is involved in the regulation of gene expression and gene silencing.[62,63] Moreover, ^{m}C is believed to cause about one third of all transition mutations responsible for human genetic diseases and cancer.[64] Therefore, it has become clinically important to know the methylation status at specific sites in genomic DNA. There are many reports mapping methylation patterns in genomic DNA using the Maxam and Gilbert chemical modification or the PCR after sodium bisulfite-mediated conversion of C to U. However, the development of a simpler and more convenient method for the site-specific discrimination of C methylation is imperative for genomic studies.

We developed a simple method for the discrimination of C and ^{m}C in duplex DNA using PNAs (Fig. 13).[65,66] This is the direct method for detecting ^{m}C site-specifically in duplex DNA. We designed the detection method using a complex produced by PNA-assisted DNA displacement in combination with FRET. Duplex DNA containing C at the target site was incubated with two complementary PNAs to displace the DNA strand, and the DNA target site was displaced as a "P-loop."[67] Subsequently, a fluorescent probe DNA, with fluorescein attached to the 5′ end and a dabsyl group to the 3′ end as a quencher, was added to hybridize with the P-loop to produce a

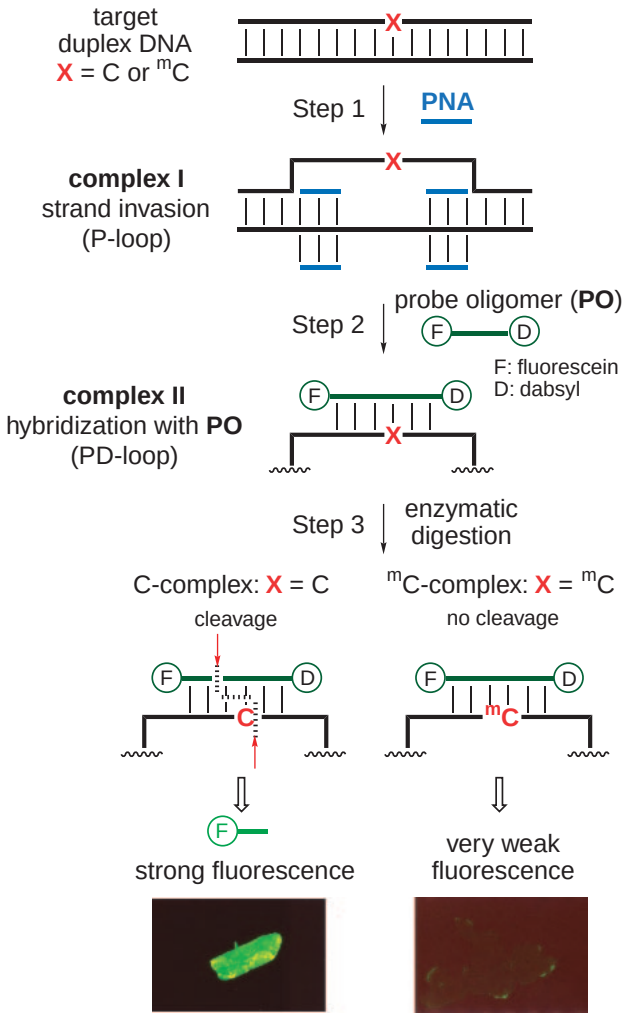

Fig. 13. The protocol for site-specific discrimination of C and ^{m}C in duplex DNA. Step 1: strand invasion of target duplex DNA by PNAs. Step 2: hybridization of the displaced DNA strand with probe oligomer. Step 3: specific cleavage by restriction enzyme. "F" and "D" of the probe oligomer denote fluorescein and dabsyl groups, respectively. The gel slice containing the *Hha*I-digested complex was observed microscopically to detect cytosine methylation.

fluorescently labeled duplex, "PD-loop."[67] The resulting complex was further treated with the appropriate restriction enzymes such as *Hha*I. The duplex containing C at the target site should produce a strong fluorescence emission when the probe DNA is digested, whereas little or no fluorescence emission should be observed with the duplex containing ^{m}C at the target site because ^{m}C inhibits digestion by the restriction enzyme. After treatment with a restriction enzyme, a strong fluorescence emission was observed with the complex containing C in the target sequence, whereas the fluorescence intensity for the complex containing ^{m}C was extremely weak. As compared with currently available methods for evaluating the methylation status of DNA, a major advantage of our method is that C methylation can be detected optically and sequence-selectively without time-consuming procedures, such as duplex denaturation and electrophoresis, although the general utility of our methods is limited by the sequence restrictions imposed on the target sequences and the well-described limitations for duplex invasion by PNAs. Site-specific discrimination of C methylation using the PD-loop complex is extremely simple compared with other ^{m}C detection methods.

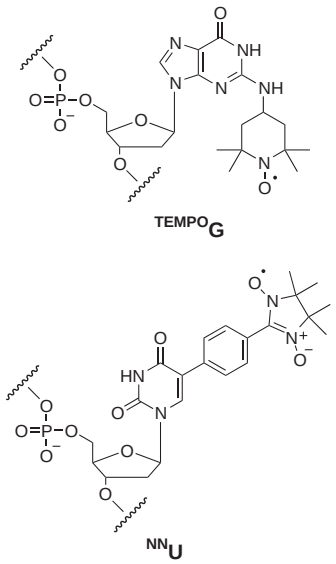

Fig. 14. Structures of spin-labeled nucleosides.

Deoxynucleosides and Oligodeoxynucleotides that Send Different Signals Depending on the Microenvironment

Spin-Labeled Nucleosides. Recent progress in spin labeling techniques have made ESR a promising technique for investigating many biological systems. In particular, site-directed spin labeling (SDSL) is emerging as a powerful technique for exploring the structure and dynamics of biomolecules.[68] The SDSL technique of labeled biomolecules provides a lot of information on the dynamics of the nitroxide group, the collision rate between a nitroxide group and a freely diffusing paramagnetic agent, and the distance between a nitroxide group and other paramagnetic species fixed in the biomolecular structure. Several nucleosides labeled with nitroxide radicals, such as 2,2,6,6-tetramethylpiperidine 1-oxyl (TEMPO) and 2,2,5,5-tetramethylpyrrolidine 1-oxyl, have been developed to analyze DNA structures and DNA–protein interactions.[69–72] We developed a guanine derivative that is equipped with a nitroxide spin label (Fig. 14).[73] ODNs containing a guanine base to which TEMPO is covalently linked (^{TEMPO}G) were synthesized, and a quadruplex structure was probed by ESR spectroscopy using a fragment ODN of the human telomere sequence containing ^{TEMPO}G. The nitroxide group in the ODN protrudes outside of the groove when the ODN forms a quadruplex in the presence of potassium ions. The hyperfine coupling constant a_N obtained from the ESR spectrum of the quadruplex in the presence of potassium ions was 17.0 G, which did not change from that of the single-stranded state in the absence of potassium ions ($a_N = 17.0$ G), suggesting that the change of micropolarity is small relative to the change in the structure. On the other hand, the rotational correlation time τ_c calculated from the quadruplex (0.32 ns) slightly decreased in comparison with

that of the single-stranded state ($\tau_c = 1.56$ ns). The change in τ_c suggests that the probe mobility increased, and is probably due to the width and shallowness of the groove and compactness of the folding structure that is characteristic of telomeric DNAs.

We also developed a novel nucleoside labeled with a nitronyl nitroxide group, ^{NN}U, and synthesized ODNs containing ^{NN}U.[74] There is still no precedent for nucleosides labeled with a nitronyl nitroxide group, which are known to be a key structure of the nitric oxide (NO) scavenger, 2-phenyl-4,4,5,5-tetramethylimidazoline-3-oxide 1-oxyl (PTIO).[75,76] When nitronyl nitroxides are incorporated into selected DNA sites, they are expected to provide a powerful new SDSL method, as well as being an NO trap. The ESR spectrum of the single-stranded ^{NN}U-containing ODN exhibited the characteristic five-line pattern, with a typical hyperfine coupling constant of $a_N = 8.21$ G, whereas the value of a_N for the spin probe in the duplex (8.25 G) was slightly higher than that of the single-stranded state. This result reflects the increased micropolarity at the binding site of the nitronyl nitroxide group in the major groove of the duplex. In addition, the duplex formation caused line broadening. This line broadening is attributed to the motion restriction of the ^{NN}U spin label within the duplex DNA. The spin signals from the ^{NN}U-containing ODNs varied because of the degree of hybridization of the complementary strand. Therefore, ^{NN}U spin labels will also be useful as a powerful SDSL tool for exploring the structure and dynamics of nucleic acids.

Monitoring of the Structural Transition of G-Rich DNA by Fluorescence-Labeled G. G-rich DNA sequences are known to adopt various structures, such as B-DNA duplex, Z-DNA duplex, and parallel and antiparallel quadruplexes, which are biologically significant and structurally interesting.[77] Well-designed fluorescent probes could provide useful information on such a conformational transition of G-rich DNA. We designed a guanine derivative in which a pyrene chromophore is tethered to C8 of guanine, ^{8Py}G (Fig. 15).[78] ^{8Py}G will be an effective fluorescent probe for the detection of a unique structure of G-rich DNA that contains a *syn* conformation at the *N*-glycosyl bond, because the bulky substituent at C8 of guanine will make a *syn* conformation at the *N*-glycosyl bond predominant. We incorporated ^{8Py}G into the sequence $d(T_3G_2)_4$, which is known to form a stable quadruplex structure in the presence of potassium ions.[79] The quadruplex state of the resulting ^{8Py}G-containing ODN showed a strong fluorescence at 458 nm ($\Phi_F = 0.116$) which seemed to derive from the exciplex between pyrene and nucleobases. When the quadruplex was converted to a single-stranded state by heating, the fluorescence wavelength was shifted to 505 nm, which corresponds to a pyrene excimer fluorescence. On the other hand, the duplex formed by the addition of the complementary strand showed only very weak monomer fluorescence at 428 and 405 nm ($\Phi_F = 0.007$). These results show that three structures of the ^{8Py}G-containing ODN, single strand–duplex–quadruplex, are distinguishable by monitoring the change of the fluorescence wavelength and the intensity of ^{8Py}G. The weak fluorescence observed for the duplex state was easily converted to strong fluorescence by removing the complementary strand. For example, the fluorescence of **ODN1** quadruplex

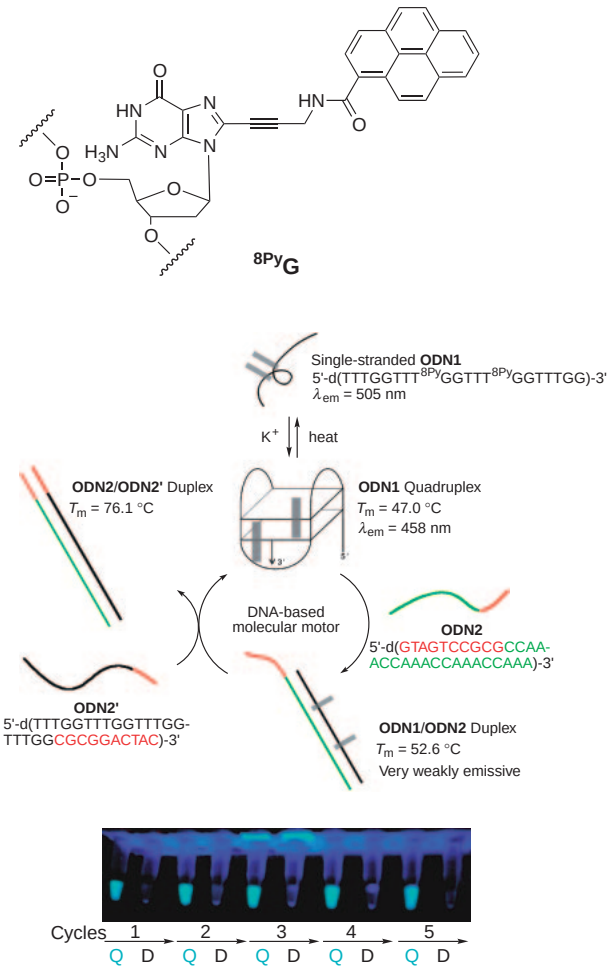

Fig. 15. Blinking of the fluorescence of ^{8Py}G-containing ODN using the DNA-based molecular motor system. Sample solutions were illuminated with a 366 nm transilluminator. Q = **ODN1** quadruplex, D = **ODN1**/**ODN2** duplex.

was rapidly quenched by mixing with the 5′-overhanged complementary strand, **ODN2** (Fig. 15). However, by the addition of the fully complementary strand of **ODN2** (**ODN2′**), **ODN2** was removed from **ODN1** to give the **ODN2**/**ODN2′** duplex, and the fluorescence of **ODN1** at 458 nm recovered rapidly. These ODNs behaved as a DNA-based molecular motor that was driven by thermodynamic demand,[80] and the fluorescence of **ODN1** blinked once for each of cycles.

Additionally, we have designed a new system for fluorometrically monitoring the transition between B- and Z-DNA by using the combination of two pyrene-labeled nucleosides, ^{Pet}G and ^{Py}C (Fig. 16).[81] ^{Pet}G, which is tethered to the C8 position via an ethynyl linker, is a fluorescent nucleoside for inducing a unique structure of G-rich DNA that contains a *syn* conformation at the *N*-glycosyl bond, as described for ^{8Py}G. In B-DNA, the two pyrenes of ^{Pet}G and ^{Py}C in a 5′-d(^{Pet}G^{Py}C)-3′/5′-d(GC)-3′ duplex are far apart, because the pyrene group of ^{Py}C is located at the major groove and the pyrene group of ^{Pet}G at the minor groove of the duplex as a result of the predominant *syn* conformation. On the other hand, in Z-DNA, where the bases alternate from G with a *syn* conformation to C with an

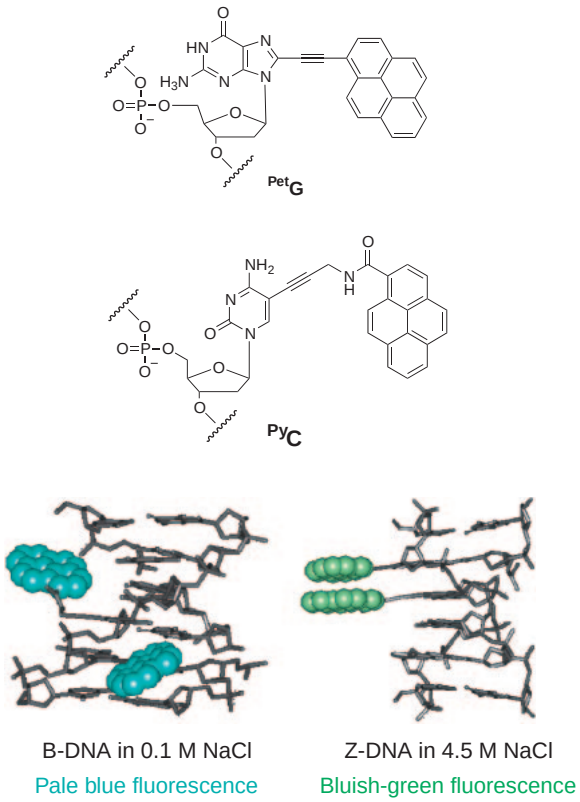

Fig. 16. Structure of ^{Pet}G and ^{Py}C, and B- and Z-structures of a DNA containing ^{Pet}G and ^{Py}C.

anti conformation, both pyrenes of a 5′-d(^{Pet}G^{Py}C)-3′/5′-d(GC)-3′ duplex are located at the same groove, and are stacked together very closely.

For example, for the self-complementary Z-DNA 5′-d(CGCGCGC^{Pet}G^{Py}CGCG)-3′ at high salt concentration, a fluorescence was observed at 507 nm upon excitation at 350 nm ($\Phi_F = 0.028$). The fluorescence wavelength from the DNA duplex was much longer than those from singly labeled ODNs, 5′-d(CGCGCGCGC^{Pet}GCGCG)-3′ ($\lambda_{max} = 400, 420$ nm; $\varepsilon_{350} = 10800$; $\varepsilon_{420} = 30000$; $\lambda_{fl} = 438$ nm; $\Phi_F = 0.06$) and 5′-d(CGCGCGCGCG^{Py}CGCG)-3′ (λ_{max} 345 nm; $\varepsilon_{350} = 16200$; $\varepsilon_{420} \sim 0$; $\lambda_{fl} = 400$ nm; $\Phi_F = 0.10$). This fluorescence wavelength was very close to that of a typical pyrene excimer, suggesting that the excited complex of ^{Pet}G and ^{Py}C was formed in the duplex. On the other hand, the B-form 5′-d(CGCGCGCGC^{Pet}G-^{Py}CGCG)-3′ at low salt concentration showed a fluorescence at 438 nm ($\Phi_F = 0.033$). Although the duplex was excited at 350 nm, which is where ^{Py}C was excited, the fluorescence at 400 nm originating from ^{Py}C was not observed, and only the fluorescence emission at 438 nm, arising from ^{Pet}G, was observed. This fluorescence wavelength indicates that the fluorescent emission via fluorescence resonance energy transfer from ^{Py}C to ^{Pet}G occurred in B-DNA. The transition between B- and Z-form structures induced by concentrations of salt is easily monitored by observing the change in the fluorescence wavelength.

Control of Drug Release by a DNA Structural Transition. DNA hybridization biosensors offer considerable promise for obtaining sequence information of genes in a fast and simple manner. Various DNA probes that give signals in a sequence-specific fashion, as represented by molecular beacons, have been widely used.[82,83] However, there are very few DNA probes that release functional molecules on recognition of their target sequence.[84] The sequence-specific molecule-releasing system that is triggered by external stimulation, such as by photoirradiation, is a very powerful alternative for gene analysis.

We designed a molecule-releasing system controllable by an intramolecular quenching based on a molecular beacon strategy using photoactive probe ODNs (Fig. 17).[85] Phenacyl ester as a photocleavable group via a triplet excited state and substituted naphthalene as a triplet quencher were incorporated into the 3′- and 5′-ends of the ODN, respectively. Using this ODN, we investigated the efficiency of the photoreaction by 312 nm irradiation before and after hybridization with the complementary DNA. Conversion of the closed form was only 5% at 0 °C for 10-s photoirradiation, whereas photoirradiation of the open form hybridized with the complementary strand resulted in a rapid degradation (25% conversion). The structural change caused by hybridization with the complementary DNA strongly affects the consumption of ODN. The stem of the closed form keeps a phenacyl ester and a naphthalene ring in close proximity to each other causing the efficient triplet quenching. In contrast, when the probe ODN is transformed to the open form by DNA hybridization, photocleavage of the phenacyl ester proceeds very smoothly under photoirradiation conditions because the photoactive phenacyl ester is far away from the naphthalene quencher.

The biotin that was released from photoactive probe ODNs by the photolysis of the phenacyl ester was quantified by mixing the photoproduct mixture with a solution of the avidin-HABA complex.[86,87] Photoirradiation of the closed form resulted in a slight decrease of A_{500}, corresponding to a 12% biotin release. In contrast, a drastic decrease of A_{500} corresponding to a 84% biotin release was observed in the presence of the complementary ODN. The efficiency of biotin releases were significantly altered by the conformational change of ODN by hybridization with the target DNA sequence.

Conclusion

We have described several examples of highly functional nucleic acids and their application to DNA technology. Unique characteristics possessed inherently by DNA, such as base pair formation, structural transition by external stimulation, and hole transport through the π-stacking of bases, have been applied to the design of highly functional nucleic acids. We spatially arranged novel functional bases in the nucleic acid structure, and activated and suppressed various functions of the synthetic nucleic acids by sequence, change of microstructure and micropolarity, and modulation of interfunctional interaction. The development of such conceptually new functional nucleic acids by means of organic synthesis could open up a new field of genome science and nanobiomaterial science.

I would like to express my sincere gratitude to Professor Isao Saito for his guidance and discussion, and to all collaborators in the Saito laboratory at Kyoto University for their efforts in contributing to these studies.

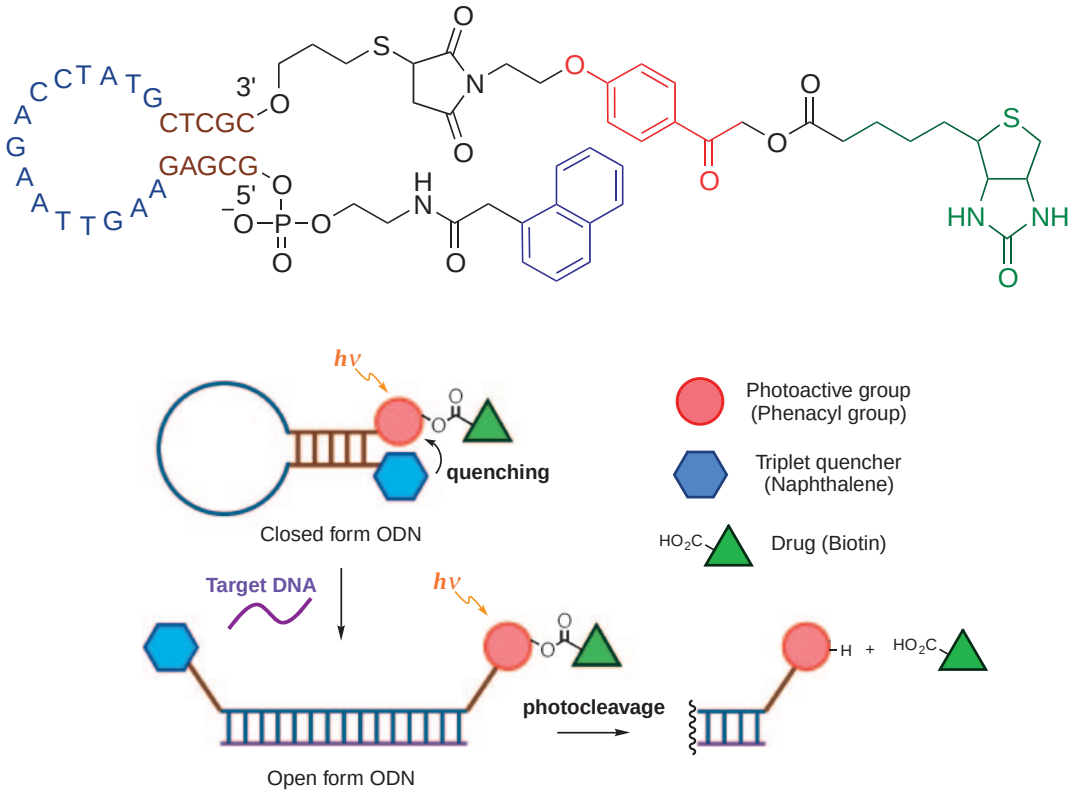

Fig. 17. Outline for the phototriggered drug release from a photocleavable ODN controlled by a molecular beacon strategy.

References

1 N. C. Seeman, *Nature*, **421**, 427 (2003).
2 N. C. Seeman, *Chem. Biol.*, **10**, 1151 (2003).
3 J. Clark, E. M. Singer, D. R. Korns, and S. S. Smith, *Biotechniques*, **36**, 992 (2003).
4 H.-W. Fink and C. Schönenberger, *Nature*, **398**, 407 (1999).
5 D. Porath, A. Bezryadin, S. de Vries, and C. Dekker, *Nature*, **403**, 635 (2000).
6 L. Cai, H. Tabata, and T. Kawai, *Appl. Phys. Lett.*, **77**, 3105 (2000).
7 D. B. Hall, R. E. Holmlin, and J. K. Barton, *Nature*, **382**, 731 (1996).
8 G. B. Schuster, *Acc. Chem. Res.*, **33**, 253 (2000).
9 B. Giese, *Acc. Chem. Res.*, **33**, 631 (2000).
10 F. D. Lewis, R. L. Letsinger, and M. R. Wasielewski, *Acc. Chem. Res.*, **34**, 159 (2001).
11 M. A. Warpehoski and L. H. Hurley, *Chem. Res. Toxicol.*, **1**, 315 (1988).
12 I. Saito, T. Nakamura, K. Nakatani, Y. Yoshioka, K. Yamaguchi, and H. Sugiyama, *J. Am. Chem. Soc.*, **120**, 12686 (1998).
13 A. Okamoto, K. Kanatani, T. Taiji, and I. Saito, *J. Am. Chem. Soc.*, **125**, 1172 (2003).
14 Q. Zhu and P. R. LeBreton, *J. Am. Chem. Soc.*, **122**, 12824 (2000).
15 A. Okamoto, K. Tanaka, and I. Saito, *J. Am. Chem. Soc.*, **125**, 5066 (2003).
16 K. Nakatani, C. Dohno, and I. Saito, *J. Am. Chem. Soc.*, **122**, 5893 (2000).
17 C. R. Treadway, M. G. Hill, and J. K. Barton, *Chem. Phys.*, **281**, 409 (2002).
18 E. T. Kool, *Curr. Opin. Chem. Biol.*, **4**, 602 (2000).
19 H. Sawai, A. N. Ozaki, F. Satoh, T. Ohbayashi, M. M. Masud, and H. Ozaki, *Chem. Commun.*, **2001**, 2604.
20 A. Okamoto, K. Tanaka, K.-i. Nishiza, and I. Saito, *Bioorg. Med. Chem.*, **12**, 5875 (2004).
21 S. Tabor and C. C. Richardson, *Proc. Natl. Acad. Sci. U.S.A.*, **86**, 4076 (1989).
22 A. Okamoto, K. Tanaka, and I. Saito, *J. Am. Chem. Soc.*, **126**, 9458 (2004).
23 T. L. Floyd, "Digital Fundamentals," 8th ed, Pearson Education, Inc., Upper Saddle River, NJ (2003).
24 A. Okamoto, K. Tanaka, and I. Saito, *Bioorg. Med. Chem. Lett.*, **12**, 97 (2002).
25 A. Okamoto, K. Tanaka, and I. Saito, *Bioorg. Med. Chem. Lett.*, **12**, 3641 (2002).
26 P. E. Nielsen, M. Egholm, and O. Buchardt, *Science*, **254**, 1497 (1991).
27 M. Egholm, O. Buchardt, L. Christensen, C. Behrens, S. M. Freier, D. A. Driver, R. H. Berg, S. K. Kim, B. Nordén, and P. E. Nielsen, *Nature*, **365**, 566 (1993).
28 A. Okamoto, K. Tanabe, C. Dohno, and I. Saito, *Bioorg. Med. Chem.*, **10**, 713 (2002).
29 E. Selsing, R. D. Wells, C. J. Alden, and S. Arnott, *J. Biol. Chem.*, **254**, 5417 (1979).
30 A. Okamoto, K. Tanaka, and I. Saito, *J. Am. Chem. Soc.*, **126**, 416 (2004).
31 H. Ikeda and I. Saito, *J. Am. Chem. Soc.*, **121**, 10836 (1999).
32 J. Cadet, M. Berger, G. W. Buchko, P. C. Joshi, S. Raoul, and J.-L. Ravanat, *J. Am. Chem. Soc.*, **116**, 7403 (1994).
33 H. Imahori and S. Fukuzumi, *Adv. Mater.*, **13**, 1197 (2001).

34 M. Lahav, V. Heleg-Shabtai, J. Wasserman, E. Katz, I. Willner, H. Dürr, Y.-Z. Hu, and S. H. Bossmann, *J. Am. Chem. Soc.*, **122**, 11480 (2000).
35 M. A. Fox, *Acc. Chem. Res.*, **32**, 201 (1999).
36 A. Okamoto, T. Kamei, K. Tanaka, and I. Saito, *J. Am. Chem. Soc.*, **126**, 14732 (2004).
37 D. G. Wang, J.-B. Fan, C.-J. Siao, A. Berno, P. Young, R. Sapolsky, G. Ghandour, N. Perkins, E. Winchester, J. Spencer, L. Kruglyak, L. Stein, L. Hsie, T. Topaloglou, E. Hubbell, E. Robinson, M. Mittmann, M. S. Morris, N. Shen, D. Kilburn, J. Rioux, C. Nusbaum, S. Rozen, T. J. Hudson, R. Lipshutz, M. Chee, and E. S. Lander, *Science*, **280**, 1077 (1998).
38 H. Haga, Y. Yamada, Y. Ohnishi, Y. Nakamura, and T. Tanaka, *J. Hum. Genet.*, **47**, 605 (2002).
39 S. Tyagi, D. P. Bratu, and F. R. Kramer, *Nat. Biotechnol.*, **16**, 49 (1998).
40 W. M. Howell, M. Jobs, U. Gyllensten, and A. J. Brookes, *Nat. Biotechnol.*, **17**, 87 (1999).
41 J. G. Hacia, *Nat. Genet.*, **21**, 42 (1999).
42 D. Whitcombe, J. Theaker, S. P. Guy, T. Brow, and S. Little, *Nat. Biotechnol.*, **17**, 804 (1999).
43 T. Pastinen, M. Raitio, K. Lindroos, P. Tainola, L. Peltonen, and A.-C. Syvänen, *Genome Res.*, **10**, 1031 (2000).
44 P. M. Lizardi, X. Huang, Z. Zhu, P. Bray-Ward, D. C. Thomas, and D. C. Ward, *Nat. Genet.*, **19**, 225 (1998).
45 V. Lyamichev, A. L. Mast, J. G. Hall, J. R. Prudent, M. W. Kaiser, T. Takova, R. W. Kwiatkowski, T. J. Sander, M. de Arruda, D. A. Arco, B. P. Neri, and M. A. D. Brow, *Nat. Biotechnol.*, **17**, 292 (1999).
46 H. Fakhrai-Rad, N. Pourmand, and M. Ronaghi, *Hum. Mutat.*, **19**, 479 (2002).
47 I. Nazarenko, R. Pires, B. Lowe, M. Obaidy, and A. Rashtchian, *Nucleic Acids Res.*, **30**, 2089 (2002).
48 S. A. E. Marras, F. R. Kramer, and S. Tyagi, *Nucleic Acids Res.*, **30**, e122 (2002).
49 A. Okamoto, K. Tainaka, and I. Saito, *J. Am. Chem. Soc.*, **125**, 4972 (2003).
50 H. Iwasaki, N. Ota, T. Nakajima, Y. Shinohara, M. Kodaira, M. Kajita, and M. Emi, *J. Hum. Genet.*, **46**, 32 (2001).
51 A. Okamoto, K. Tainaka, and I. Saito, *Photomed. Photobiol.*, **25**, 39 (2003).
52 A. Okamoto, K. Tainaka, and I. Saito, *Chem. Lett.*, **32**, 684 (2003).
53 A. Okamoto, K. Tainaka, and I. Saito, *Tetrahedron Lett.*, **44**, 6871 (2003).
54 A. Okamoto, K. Tanaka, T. Fukuta, and I. Saito, *J. Am. Chem. Soc.*, **125**, 9296 (2003).
55 A. Okamoto, K. Tanaka, T. Fukuta, and I. Saito, *ChemBioChem*, **5**, 958 (2004).
56 A. Okamoto, K. Kanatani, and I. Saito, *J. Am. Chem. Soc.*, **126**, 4820 (2004).
57 A. P. de Silva, H. Q. N. Gunaratne, T. Gunnlaugsson, A. J. M. Huxley, C. P. McCoy, J. T. Rademacher, and T. E. Rice, *Chem. Rev.*, **97**, 1515 (1997).
58 E. P. Reddy, R. K. Reynolds, E. Santos, and M. Barbacid, *Nature*, **300**, 149 (1982).
59 A. Okamoto, T. Ichiba, and I. Saito, *J. Am. Chem. Soc.*, **126**, 8364 (2004).
60 J. H. Hansson, L. Schild, Y. Lu, T. A. Wilson, I. Gautschi, R. Shimkets, C. Nelson-Williams, B. C. Rossier, and R. P. Lifton, *Proc. Natl. Acad. Sci. U.S.A.*, **92**, 11495 (1995).
61 T. Inoue, Y. Okauchi, Y. Matsuzaki, K. Kuwajima, H. Kondo, N. Horiuchi, K. Nakao, M. Iwata, Y. Yokogoshi, Y. Shintani, H. Bando, and S. Saito, *Eur. J. Endocrinol.*, **138**, 691 (1998).
62 C. Cogoni, *Annu. Rev. Microbiol.*, **55**, 381 (2001).
63 J. Paszkowski and S. Whitham, *Curr. Opin. Plant Biol.*, **4**, 123 (2001).
64 C. H. Spruck, III, W. M. Rideout, III, and P. A. Jones, "DNA Methylation: Molecular Biology and Biological Significance," ed by J. P. Jost and H. P. Saluz, Birkhäuser Verlag, Basel, Switzerland (1993), pp. 487–509.
65 A. Okamoto, K. Tanabe, and I. Saito, *J. Am. Chem. Soc.*, **124**, 10262 (2002).
66 A. Okamoto, K. Tanabe, and I. Saito, *Bioorg. Med. Chem.*, **11**, 3747 (2003).
67 H. Kuhn, V. V. Demidov, J. M. Coull, M. J. Fiandaca, B. D. Gildea, and M. D. Frank-Kamenetskii, *J. Am. Chem. Soc.*, **124**, 1097 (2002).
68 B. H. Robinson, H. Thomann, A. H. Beth, P. Fajer, and L. R. Dalton, "EPR and Advanced EPR Studies of Biological Systems," CRC Press, New York (1985).
69 A. Spaltenstein, B. H. Robinson, and P. B. Hopkins, *J. Am. Chem. Soc.*, **110**, 1299 (1988).
70 O. K. Strobel, D. D. Kryak, E. V. Bobst, and A. M. Bobst, *Bioconjugate Chem.*, **2**, 89 (1991).
71 K. Makino, S. Nagahara, Y. Konishi, M. Mukae, H. Ide, and A. Murakami, *Free Radical Res. Commun.*, **19**, Suppl. 1, S109 (1993).
72 P. Z. Qin, K. Hideg, J. Feigon, and W. L. Hubbell, *Biochemistry*, **42**, 6772 (2003).
73 A. Okamoto, T. Inasaki, and I. Saito, *Bioorg. Med. Chem. Lett.*, **14**, 3415 (2004).
74 A. Okamoto, T. Inasaki, and I. Saito, *Tetrahedron Lett.*, **46**, 791 (2005).
75 T. Akaike, M. Yoshida, Y. Miyamoto, K. Sato, M. Kohno, K. Sasamoto, K. Miyazaki, S. Ueda, and H. Maeda, *Biochemistry*, **32**, 827 (1993).
76 Y. Yoshie and H. Ohshima, *Chem. Res. Toxicol.*, **10**, 1015 (1997).
77 V. A. Bloomfield, D. M. Crothers, and I. Tinoco, Jr., "Nucleic Acids: Structures, Properties, and Functions," University Science Books, Sausalito, CA (2000).
78 A. Okamoto, K. Kanatani, Y. Ochi, Y. Saito, and I. Saito, *Tetrahedron Lett.*, **45**, 6059 (2004).
79 E. Dias, J. L. Battiste, and J. R. Williamson, *J. Am. Chem. Soc.*, **116**, 4479 (1994).
80 B. Yurke, A. J. Turberfield, A. P. Mills, Jr., F. C. Simmel, and J. L. Neumann, *Nature*, **406**, 605 (2000).
81 A. Okamoto, Y. Ochi, and I. Saito, *Chem. Commun.*, **2005**, 1128.
82 S. Tyagi and F. R. Kramer, *Nat. Biotechnol.*, **14**, 303 (1996).
83 S. Tyagi, D. P. Btaru, and F. R. Kramer, *Nat. Biotechnol.*, **16**, 49 (1998).
84 Z. Ma and J.-S. Taylor, *Proc. Natl. Acad. Sci. U.S.A.*, **97**, 11159 (2000).
85 A. Okamoto, K. Tanabe, T. Inasaki, and I. Saito, *Angew. Chem., Int. Ed.*, **42**, 2502 (2003).
86 N. M. Green, *Biochem. J.*, **94**, 23c (1965).
87 H. Hofstetter, M. Morpurgo, O. Hofstetter, E. A. Bayer, and M. Wilchek, *Anal. Biochem.*, **284**, 354 (2000).

Dr. Akimitsu Okamoto was born in Nagoya, Japan, in 1970. He received his B.S. (1993), M.S. (1995), and Ph.D. (1998) degrees from Kyoto University. In 1998–1999, he performed postdoctoral research at Massachusetts Institute of Technology. In 1999, he joined the Department of Synthetic Chemistry and Biological Chemistry, Faculty of Engineering, Kyoto University, as an assistant professor and started his research on functional nucleic acid chemistry. In 2005, he received the Chemical Society of Japan Award for Young Chemists for 2004. His current researches have focused on the development of highly functional biomolecules and their application to life science.